IPC
Indonesian Physics Communication
Department of Physics, Universitas Riau, Pekanbaru, Indonesia
p-ISSN 1412-2960 | e-ISSN 2579-521X
Vol. 21 | No. 3
November 2024
Web: https://kfi.ejournal.unri.ac.id
E-mail: kfi@ejournal.unri.ac.id

N-doped porous activated carbon from rubber seed shells (*Hevea brasiliensis*) as high-energy supercapacitor material

Siti Rahma Daulay, Rakhmawati Farma, Awitdrus*
Department of Physics, Universitas Riau, Pekanbaru 28293, Indonesia

*Corresponding author: awitdrus@lecturer.unri.ac.id

ABSTRACT

Biomass is an environmentally safe and cost-effective source of activated carbon (AC) for supercapacitors (SC). In this study, AC was generated using precarbonisation and activation with KOH using rubber seed shell (RSS) as a precursor. The electrochemical performance was investigated by cyclic voltammetry and galvanostatic charge-discharge determination and the ACs were characterised using FTIR analysis technique. RSS materials were prepared by varying calcination temperatures of 700°C, 800°C, and 900°C without doping. RSS_{800} shows a maximum specific capacitance of 190 F/g and has an energy density of 26.2 Wh/kg and a power density of 695.4 kW/kg at 1 A/g. Furthermore, melamine was used as an external dopant source for the N-doping process. The doped AC sample (RSS_{800-90}) had a specific capacitance of 288 F/g and has an energy density of 40.9 Wh/kg and a power density of 515.4 kW/kg at 1 A/g in H_2SO_4 electrolyte. N-doped with melamine as nitrogen source was successfully incorporated into AC to produce high-performance electrodes for SC.

Keywords: Activated carbon; KOH; N-doped; rubber seed shell; supercapacitors

Received 06-09-2023 | Revised 17-10-2023 | Accepted 04-11-2024 | Published 30-11-2024

INTRODUCTION

The knowledge and demand for energy storage systems that are efficient, sustainable and environmentally friendly is increasing due to technological advancements in various industrial sectors, so the exploration of renewable energy sources that are environmentally friendly is essential for the long-term economic growth of society [1, 2]. Supercapacitors (SC) are one that has attracted great attention as an environmentally friendly, efficient and effective option because they have excellent power density and a long lifetime [3].

In general, electrode materials for SC include activated carbon (AC), metal oxides, polymers, graphene, etc. AC has proven to be an excellent electrode material when compared to other types of carbon materials. Environmental pollution and the depletion of fossil fuel reserves are the reasons why researchers are exploring biomass waste as a potential alternative for producing AC. Various biomass wastes such as wood [4], empty oil palm sign [5], coconut shells [6], eggshells [7], has been converted to AC to serve as the electrode material for SC.

AC can be produced using physico-chemical activation techniques. In the chemical activation technique, biomass as a precursor will be combined with chemical activators, such as H_2SO_4, H_3PO_4, KOH, NaOH, and $ZnCl_2$ [8, 9]. Compared to other activating agents, KOH is one of the most effective and environmentally friendly, making it more ideal for use in the chemical activation process for AC manufacturing [9, 10]. Physical activation techniques can be performed using oxidising agents, such as carbon dioxide (CO_2), water vapour, air, or a combination of these gases. CO_2 is often chosen as an activation agent due to its safe and contains no toxins nature [11]. Activation temperature, the amount of activating agent, as well as heat pretreatment, all affect porosity formation during the activation process using KOH and CO_2 [12]. Heteroatom doping is one way to increase the energy storage capacity of carbon-based electrodes and improve the electron transport rate. The increase in apparent capacitance is obtained under Faraday reaction conditions while maintaining the EDLC features [13, 14].

Heteroatoms can be introduced into the AC framework by changing the electron distribution and bonding properties of the surrounding carbon lattice. Elements such as N, P, S, and B are added into the carbon structure to modify its Fermi level shift and electronic structure [15, 16]. In addition, heteroatom functional groups not only reduce the resistance to charge transfer at the electrode, but also increase the wettability of the carbon network to improve the performance of the material. Nitrogen-doped carbon can be synthesised via thermal methods using nitrogen-containing compounds, such as ammonia gas (NH_3), melamine, urea, and acetonitrile [17].

Melamine-based nitrogen doping has been investigated to improve the performance of SC electrodes. For instance, Tran et al., successfully used the melamine as a nitrogen source synthesis of activated carbon from oil palm empty fruit bunches and its modification with nitrogen doping for supercapacitor applications a specific capacitance 182 to 217 F/g [18]. Kong et al. (2024), N doped porous carbon synthesised via Lewis acid salt activation for supercapacitors with high rate performance of 234 F/g [19].

Rubber seed shell (*Hevea brasiliensis*) is one of the flowering plants of the Moraceae family endemic to the eastern part of Southeast Asia and South Asia. Rubber seed shell (RSS) consists of 48.64% cellulose, 33.54% lignin, and 18.0% hemicellulose. However, RSS is often dumped on the ground and decomposes without optimal utilisation, resulting in a large amount of waste. Therefore, RSS was chosen as a carbon precursor for the manufacture of AC as a SC electrode in this study. This study aims to produce activated carbon from Hevea brasiliensis biomass through a combination of one-stage activation techniques using KOH and CO_2, and implement it as an electrode material for supercapacitors.

MATERIALS AND METHODS

RSS waste was collected from Sidokan Panompuan Village, Padang Lawas Regency, North Sumatra Province. The RSS was cleaned using deionised water to remove impurities, then dried in the sun for 5 days, followed by oven drying for 2 days. Next, the RSS was carbonised at 250°C for 3 hours, pulverised using ball milling to obtain fine powder, and sieved to a size of 53 µm. A total of 30 g of activated carbon powder was then activated with 150 ml of 0.5 M KOH solution and heated for 2 hours. The activated samples were cooled to room temperature, then dried in an electric oven overnight. After drying, the samples were shaped into coins and put into a horizontal furnace for activation at 700°C under CO_2 gas flow. The product is washed to a neutral pH (pH~7) and labelled as RSS_{700}. By repeating the same steps, activation was carried out at 800°C and 900°C, which were labelled as RSS_{800} and RSS_{900}, respectively. By repeating the steps, 0.3 g of melamine was dissolved in 100 ml of deionised water and heated for 10 minutes. In the doping process, 20 coin samples were immersed in the solution for 24 hours and dried overnight. Next, the dried coin samples were heated at 300°C in an N_2 atmosphere for different times (60, 90, and 120 minutes). The resulting products were labelled as RSS_{800-60}, RSS_{800-90}, and $RSS_{800-120}$.

RESULTS AND DISCUSSION

Fourier Transform Infrared Spectroscopy

Infrared spectroscopy is the most commonly used spectroscopic technique to measure the IR frequencies of AC chemical functional groups. In Figures 1 (a) and (b) shows, the vibrations detected on activated carbon are: C=C=C stretching vibrations at 2109 – 2114 cm^{-1}, C=C bond stretching vibrations (in alkynes) at 1992 – 1994 cm^{-1} [20]. The Fourier transform infrared spectroscopy (FTIR) spectrum shows a relatively weak signal with several bands in the 1500 – 2000 cm^{-1} range, which are usually associated with C–C and C=O stretching, as is often found in almost pure amorphous carbon [21] before and after N-doped using melamine that changes only the wavelength.

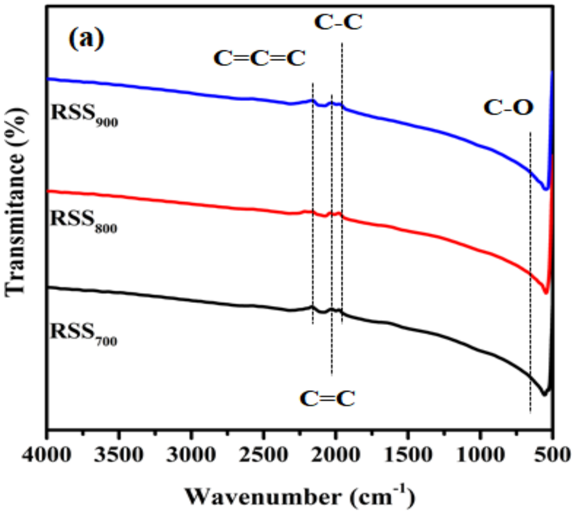

(a)

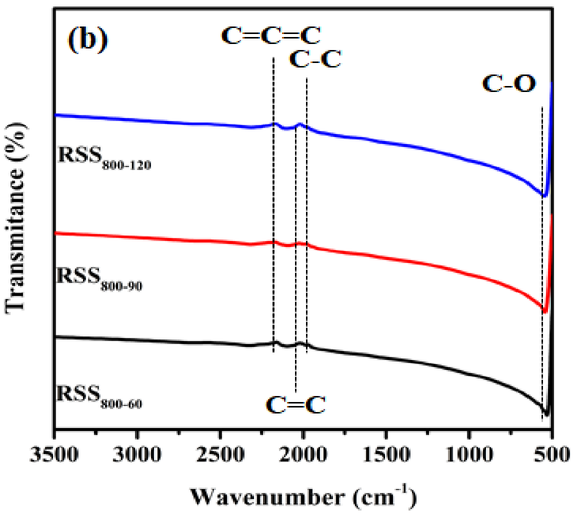

(b)

Figure 1. FTIR: (a) before N-doped; (b) and after N-doped.

Cyclic Voltammetry

Cyclic voltammetry (CV) is a method used to determine the electrochemical properties and capacitance value of an electrode by providing a voltage variation at each unit time. The electrochemical characteristics of the RSS electrode without doping are shown in Figure 2(a), the highest capacitance value is found in RSS_{800} which is a normal rectangular shape showing typical electric double layer capacitance (EDLC) behaviour. The CV curve shows the quasi-rectangular shape of the current response on reversal. Voltage without obvious redox peaks which confirm the good EDLC character of the electrode [22]. The CV curves of RSS_{800} at various scanning speeds (1, 2, 5 and 10 mV/s) are shown in Figure 2 (b). Furthermore, the CV curves of the RSS samples after doping RSS_{800-60}, RSS_{800-90}, and $RSS_{800-120}$ Figure 2 (c) show a rectangular shape with a fairly clear redox peak, showing the merging of EDLC and pseudo-capacitance behaviour. This redox peak could be due to the doping effect of melamine as the dopant source [23]. Compared with other samples, the RSS_{800-90} curve has a larger integral area, thus indicating better electrochemical performance. The CV curves at various scanning speeds (1, 2, 5 and 10 mV/s) are shown in Figure 2 (d).

Galvanostatic Charge-Discharge

Galvanostatic charge-discharge (GCD) is one of the most useful techniques to calculate electochemical capacitance under controlled current conditions [24]. Figure 3 (a) RSS_{800} shows the GCD curve is symmetrically triangular even at high current densities, which demonstrates excellent rate capability compared to the other two electrodes [25]. The GCD curves of RSS_{800} at various curent densities (1, 2, 5, and 10 A/g) are shown in Figure 3 (b). In Figure 3 (c) all electrodes show a triangular shape with a smaller IR drop, indicating high colombic efficiency [26]. The presence of heteroatoms and surface functional groups activate various Faraday processes, which favour the functioning of the EDLC system. The longer charge and discharge duration of RSS_{800-90} indicates superior capacitive performance and is in agreement with the results of CV curve analysis. Moreover, the addition of nitrogen into the carbon structure is able to increase the moisture retention capacity and conductivity of the carbon material, which ultimately improves the electrochemical performance [27]. The GCD curves of RSS_{800-90} at at various curent densities (1, 2, 5, and 10 A/g are shown in Figure 3 (d).

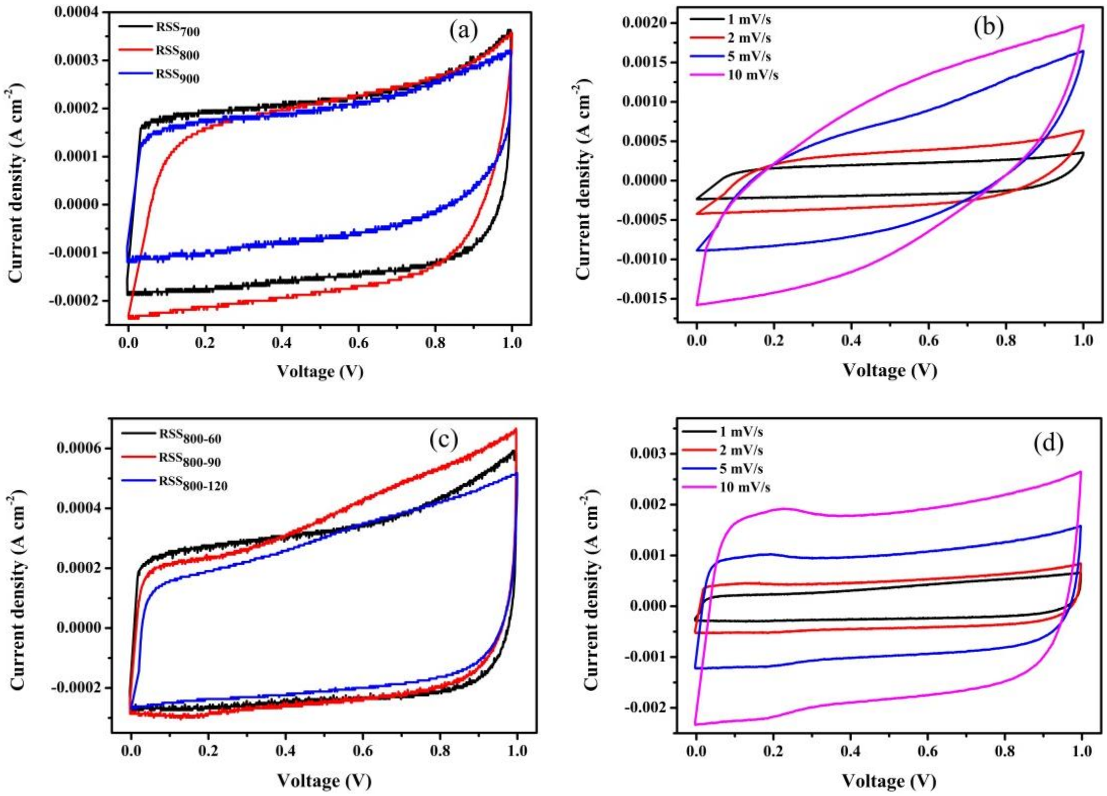

Figure 2. CV curve of: (a) RSS electrodes; (b) RSS_{800} at various scan rates; (c) RSS after N-doped electrodes; and (d) HB_{800-90} at various scan rates.

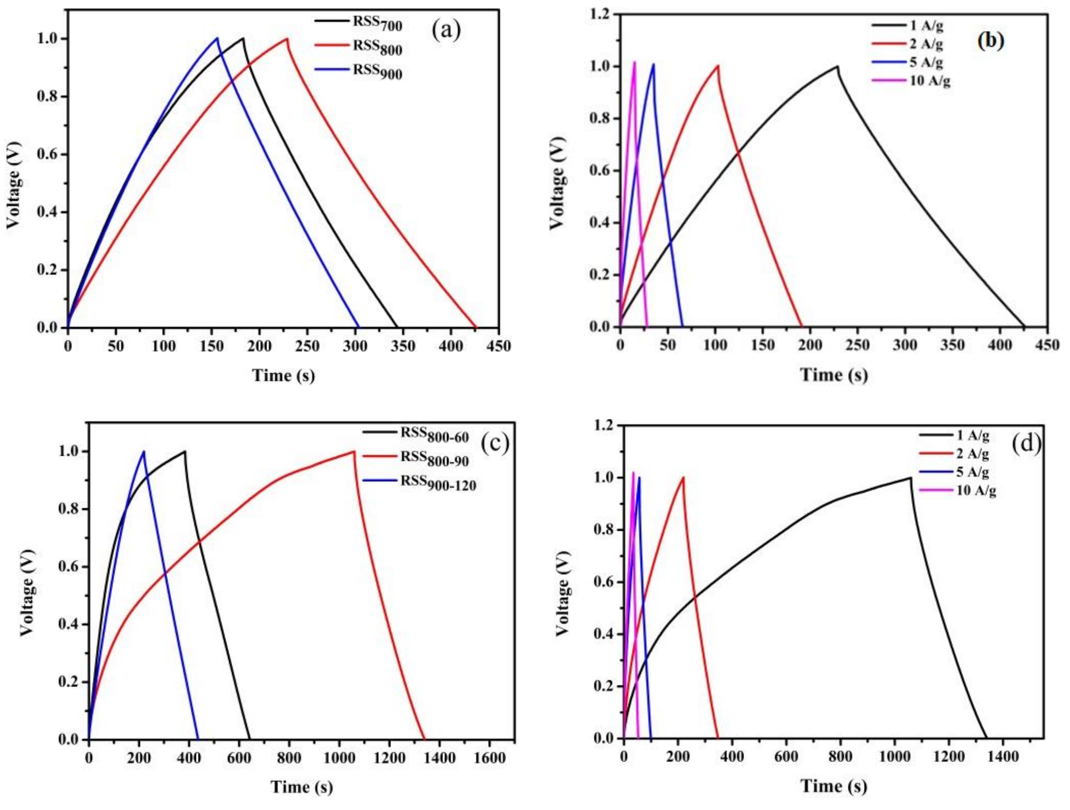

Figure 3. GCD curve of: (a) RSS electrodes; (b) RSS_{800} at various curent densities; (c) RSS after N-doped electrodes; and (d) HB_{800-90} at various curent densities.

The longer charge-discharge duration of RSS_{800-90} indicates superior capacitive performance and agrees with the CV curve analysis results. The specific capacitance (C_{sp}), energy density (E_d), and power density (P_d) are obtained from the GCD curve and calculated using specific formulae [28, 29].

$$C_s = 2I\Delta t / m\Delta V \quad (1)$$

$$E_d = CV^2 / 7.2 \quad (2)$$

$$P_d = 3600 \frac{E}{\Delta t} \quad (3)$$

where, I (A) is the discharge current, Δt (s) is the discharge duration, ΔV (V) is the potential range during discharge, and m (g) is the electrode mass. The C_{sp}, E_d, and P_d values of all RSS electrodes can be seen in Table 1.

Tabel 1. Values of specific capacitance (C_{sp}), energy density (E_d), and power density (P_d).

Sample	C_{sp} (F/g)	P_{sp} (W/kg)	E_{sp} (Wh/kg)
RSS_{700}	165	513.3	22.9
RSS_{800}	190	695.4	26.2
RSS_{900}	151	511.7	20.9
RSS_{800-60}	266	513.8	36.8
RSS_{800-90}	288	515.4	40.9
$RSS_{800-120}$	220	510.2	30.6

CONCLUSION

Biomass activated carbon derived from rubber seed shells through the combination of heteroatom doping has been successfully fabricated and analysed. In addition, melamine used as an external dopant source for N doping process can improve the capacitive behaviour of SC. AC without doping treatment (RSS_{800}) has a specific capacitance of 190 F/g and AC with doping treatment ($RSS_{800-900}$) has a specific capacitance of 288 F/g at 1 A/g, respectively. In summary, N-doped with melamine as nitrogen source was successfully incorporated into AC to improve the capacitive properties of the electrode. This research may provide a new approach for the fabrication of N-doped ACs using external dopant sources and implemented as SC electrode materials.

ACKNOWLEDGMENTS

The authors would like to thank DRTPM-Kemdikbudristek of the Republic of Indonesia for financial support through the 2024 master's thesis research grant (Contract No: 083/E5/PG.02.00.PL/2024 and 20721/UN.19.5.1.3/AL.04/2024).

REFERENCES

1. Han, G., Jia, J., Liu, Q., Huang, G., Xing, B., Zhang, C., & Cao, Y. (2022). Template-activated bifunctional soluble salt $ZnCl_2$ assisted synthesis of coal-based hierarchical porous carbon for high-performance supercapacitors. *Carbon*, **186**, 380–390.
2. Yi, E., Shen, X., Chen, X., Jiang, M., Yan, W., Liu, Y., Jiang, W., & Abdullah, M. (2023). Preparation of biomass composite activated carbon based supercapacitor materials and their application in energy storage devices. *Chemical Engineering Science*, **282**, 119193.
3. Du, X., Lin, Z., Zhang, Y., & Li, P. (2023). Microstructural tailoring of porous few-layer graphene-like biochar from kitchen waste hydrolysis residue in molten carbonate medium: Structural evolution and conductive additive-free supercapacitor application. *Science of The Total Environment*, **871**, 162045.
4. Ouyang, J., Wang, X., Wang, L., Xiong, W., Li, M., Hua, Z., Zhao, L., Zhou, C., Liu, X., Chen, H., & Luo, Y. (2022). Construction of a porous carbon skeleton in wood tracheids to enhance charge

storage for high-performance supercapacitors. *Carbon*, **196**, 532–539.

5. Rustamaji, H., Prakoso, T., Devianto, H., & Widiatmoko, P. (2023). Parameter study in preparation of nitrogen-rich-activated carbon for supercapacitors' application using multilevel factorial design. *Materials Today: Proceedings*, **3**(4),163.
6. Keppetipola, N. M., Dissanayake, M., Dissanayake, P., Karunarathne, B., Dourges, M. A., Talaga, D., Servant, L., Olivier, C., Toupance, T., Uchida, S., Tennakone, K., & Cojocaru, L. (2021). Graphite-type activated carbon from coconut shell: a natural source for eco-friendly non-volatile storage devices. *RSC advances*, **11**(5), 2854–2865.
7. Pant, B., Ojha, G. P., Acharya, J., & Park, M. (2023). Preparation, characterization, and electrochemical performances of activated carbon derived from the flower of *Bauhinia variegata L.* for supercapacitor applications. *Diamond and Related Materials*, **136**, 110040.
8. Aruchamy, K., Dharmalingam, K., Lee, C. W., Mondal, D., & Kotrappanavar, N. S. (2022). Creating ultrahigh surface area functional carbon from biomass for high performance supercapacitor and facile removal of emerging pollutants. *Chemical Engineering Journal*, **427**, 131477.
9. Wu, W., Zheng, H., Zhang, Y., Wang, Q., Huang, W., Xiang, J., Yang, X., Lu, W., Zhang, Z., & Wang, S. (2023). Preparation of high performance supercapacitors with nitrogen and oxygen self-doped porous carbon derived from wintersweet-fruit-shell. *Journal of Physics and Chemistry of Solids*, **177**, 111274.
10. Gao, Y., Yue, Q., Gao, B., & Li, A. (2020). Insight into activated carbon from different kinds of chemical activating agents: A review. *Science of the Total Environment*, **746**, 141094.
11. Xu, H., Zhang, Y., Wang, L., Chen, Y., & Gao, S. (2021). Hierarchical porous biomass-derived carbon framework with ultrahigh surface area for outstanding capacitance supercapacitor. *Renewable Energy*, **179**, 1826–1835.
12. Karakehya, N. (2023). Effects of one-step and two-step KOH activation method on the properties and supercapacitor performance of highly porous activated carbons prepared from Lycopodium clavatum spores. *Diamond and Related Materials*, **135**, 109873.
13. Gao, Y., Wang, J., Huang, Y., Zhang, S., Zhang, S., & Zou, J. (2023). Rational design of N-doped porous biomass carbon nanofiber electrodes for flexible asymmetric supercapacitors with high-performance. *Applied Surface Science*, **638**, 158137.
14. Kim, M. J., Park, J. E., Kim, S., Lim, M. S., Jin, A., Kim, O. H., Kim, M.J., Lee, K.S., Kim, J., Kim, S.S. Cho, Y.H., & Sung, Y. E. (2019). Biomass-derived air cathode materials: pore-controlled S, N-Co-doped carbon for fuel cells and metal–air batteries. *ACS catalysis*, **9**(4), 3389–3398.
15. Jerez, F., Ramos, P. B., Córdoba, V. E., Ponce, M. F., Acosta, G. G., & Bavio, M. A. (2023). Yerba mate: From waste to activated carbon for supercapacitors. *Journal of Environmental Management*, **330**, 117158.

16. Feng, T., Wang, S., Hua, Y., Zhou, P., Liu, G., Ji, K., Lin, Z., Shi, S., Jiang, X., & Zhang, R. (2021). Synthesis of biomass-derived N, O-codoped hierarchical porous carbon with large surface area for high-performance supercapacitor. *Journal of Energy Storage*, **44**, 103286.
17. Ding, Y., Li, Y., Dai, Y., Han, X., Xing, B., Zhu, L., Qiu, K., & Wang, S. (2021). A novel approach for preparing in-situ nitrogen doped carbon via pyrolysis of bean pulp for supercapacitors. *Energy*, **216**, 119227.
18. Tran Thi Dieu, H., Charoensook, K., Tai, H. C., Lin, Y. T., & Li, Y. Y. (2021). Preparation of activated carbon derived from oil palm empty fruit bunches and its modification by nitrogen doping for supercapacitors. *Journal of Porous Materials*, **28**, 9–18.
19. Kong, Q., Zhang, Q., Yan, B., Chen, J., Chen, D., Jiang, L., Lan, T., Zhang, C., Yang, W., & He, S. (2024). N/O co-doped porous carbon synthesized by lewis acid salt activation for high rate performance supercapacitor. *Journal of Energy Storage*, **80**, 110322.
20. Al, K., & Kabakcı, S. B. (2024). Oxygen-rich precursors via glycerol organosolv treatment: Preparation of activated carbon from hazelnut shell and its structural components for possible use in electrodes for supercapacitors. *International Journal of Thermofluids*, **21**, 100588.
21. Boulanger, N., Talyzin, A. V., Xiong, S., Hultberg, M., & Grimm, A. (2024). High surface area activated carbon prepared from wood-based spent mushroom substrate for supercapacitors and water treatment. *Colloids and Surfaces A: Physicochemical and Engineering Aspects*, **680**, 132684.
22. Seman, R. N. A. R., & Azam, M. A. (2020). Hybrid heterostructures of graphene and molybdenum disulfide: The structural characterization and its supercapacitive performance in 6M KOH electrolyte. *Journal of Science: Advanced Materials and Devices*, **5**(4), 554–559.
23. Zhou, Y., Ren, X., Du, Y., Jiang, Y., Wan, J., & Ma, F. (2020). In-situ template cooperated with urea to construct pectin-derived hierarchical porous carbon with optimized pore structure for supercapacitor. *Electrochimica Acta*, **355**, 136801.
24. Bhushan M. (2023). Various characterization techniques for nanomaterials. *Energy Applications*, **11**(2), 103–114.
25. Xue, B., Xu, J., & Xiao, R. (2023). Ice template-assisting activation strategy to prepare biomass-derived porous carbon cages for high-performance Zn-ion hybrid supercapacitors. *Chemical Engineering Journal*, **454**, 140192.
26. Yang, X., Wang, Q., Lai, J., Cai, Z., Lv, J., Chen, X., Chen, Y., Zheng, X., Huang, B., & Lin, G. (2020). Nitrogen-doped activated carbons via melamine-assisted NaOH/KOH/urea aqueous system for high performance supercapacitors. *Materials Chemistry and Physics*, **250**, 123201.
27. Ma, M., Zhang, J., Huan, Y., Ren, M., Wei, T., & Yan, S. (2023). 3D stack tubular mesoporous carbon derived from discarded sesame capsule shells for high-

performance supercapacitors. *Diamond and Related Materials*, *131*, 109562.

28. Xie, M., Meng, H., Chen, J., Zhang, Y., Du, C., Wan, L., & Chen, Y. (2021). High-volumetric supercapacitor performance of ordered mesoporous carbon electrodes enabled by the faradaic-active nitrogen doping and decrease of microporosity. *ACS Applied Energy Materials*, **4**(2), 1840–1850.
29. Zhang, G., Zhu, R., Zhang, R., Sun, C., & Long, Z. (2023). A novel strategy for large-scale preparation of flexible high-conductivity carbon fiber paper for supercapacitors. *Diamond and Related Materials*, **138**, 110229.